We are IntechOpen,
the world's leading publisher of
Open Access books
Built by scientists, for scientists

4,800
Open access books available

122,000
International authors and editors

135M
Downloads

Our authors are among the

154
Countries delivered to

TOP 1%
most cited scientists

12.2%
Contributors from top 500 universities

BOOK CITATION INDEX
CLARIVATE ANALYTICS
INDEXED

WEB OF SCIENCE™

Selection of our books indexed in the Book Citation Index
in Web of Science™ Core Collection (BKCI)

Interested in publishing with us?
Contact book.department@intechopen.com

Spike-Timing-Dependent Plasticity in Memristors

Yao Shuai, Xinqiang Pan and Xiangyu Sun

Additional information is available at the end of the chapter

Abstract

The spike-timing-dependent plasticity (STDP) characteristic of the memristor plays an important role in the development of neuromorphic network computing in the future. The STDP characteristics were observed in different memristors based on different kinds of materials. The investigation regarding the influences of device hysteresis characteristic, the initial conductance of the memristors, and the waveform of the voltage pulses applied to the memristor as preneuron voltage spike and postneuron voltage spike on the STDP behavior of memristors are reviewed.

Keywords: Memristor, Spike-timing-dependent plasticity

1. Introduction

The state-of-the-art artificial intelligence based on traditional von Neumann computation paradigm has shown remarkable learning and thinking abilities, for instance, AlphaGo created by the Google-owned company Deep Mind beat the top Go player Lee Sedol by 4:1 recently [1]. However, the information processing through the digital von Neumann computation paradigm is much less efficient as compared to human brains, which is the major bottleneck of von Neumann computation paradigm. Synapse plays the key role in learning, thinking, and memorizing for a human being, and there are approximately 10^{14} synapses in a human's brain [2]. A synapse is formed between two neuron cells [3], and the synapse weight can be precisely tuned by the ionic flowing through them. It is well known that the adaptation of the synapse weight between two neurons it connects with makes the biological systems functional [4]. In order to build up a system that behaves in

a much more efficient way like a human brain, people have never stopped searching for an electrical element that mimics the basic function of a synapse until "the miss memristor found [5]."

Similar to a biological synapse, memristor is a two-terminal device whose conductance can be changed by the input pulses or by controlling the charge through it [4, 6] and in such a way, a memristor works as an artificial electronic synapse. Electronic synapses based on memristor devices are around three orders of magnitude smaller than a prominent CMOS design [2]; thus, the memristor has a great potential for scalability as compared to the electronic synapse made by traditional complex circuits [7].

Synapses have different kinds of plasticity, which have been realized and investigated in different memristors [8]. And the research on the application of memristors with the common synaptic plasticity in some kind of neural networks has also been conducted. For instance, HfO_2-based memristors were used in a Hopfield neural network to implement associative memory [9]. The relationship between the resistance of the memristor and the synaptic weight was defined. And the resistances of the memristors were tuned to the target resistances through the application of the voltage pulses on the memristors as the training process [9]. Prezioso et al. realized pattern classification by using the neural network based on memristors with synaptic plasticity [10]. The 12 × 12 crossbar with Pt/Al_2O_3/TiO_{2-x}/Ti/Pt memristors at each cross point was fabricated, which is illustrated in **Figure 1(a)**. Sixty memristors among them were used to realize the function. The relationship between synaptic weight and conductance of the memristors is shown in Eq. (1). The synaptic weight was changed by applying fixed voltage pulses with the amplitude of ±1.3 V on the memristors, and the change of conductance under different voltage pulses is shown in **Figure 1(c)**.
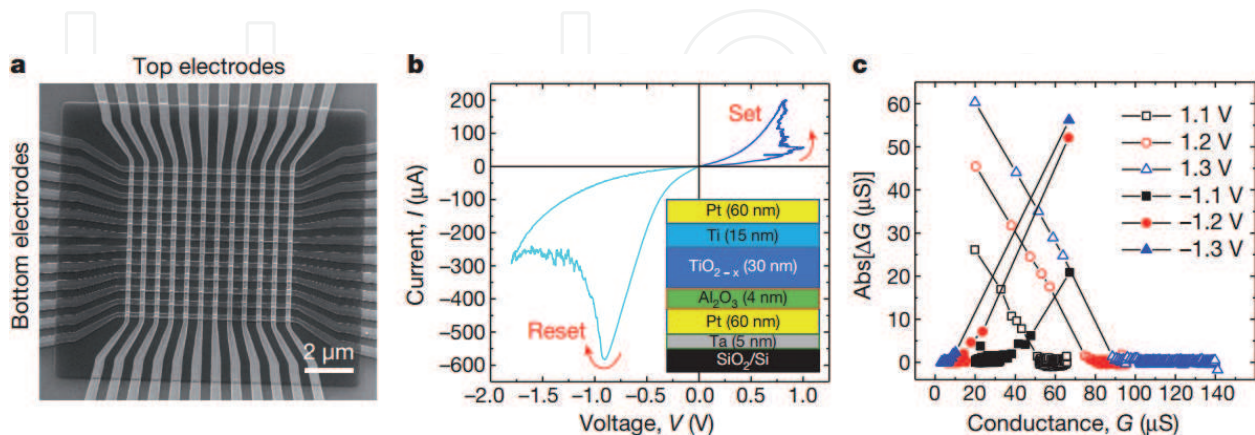
$$W_{ij} = G_{ij}^+ - G_{ij}^-$$
(1)

Figure 1. Memristor crossbar. (a) Integrated 12 × 12 crossbar with an Al_2O_3/TiO_{2-x} memristor at each cross point. (b) I–V curve of the memristor. Inset (b): the cross-sectional structure of the memristor device. (c) Absolute values of the change of memristor's conductance under voltage pulses (with the width of 500 μs) of two polarities, as a function of the initial conductance, for various pulse amplitudes [10].

2. STDP in memristors

In the common synaptic plasticity mentioned above, the change of the conductance (weight) is only related to one voltage pulse applied on the memristors. Another kind of plasticity of the synapses is spike-timing-dependent plasticity (STDP). STDP is one of the most important synaptic characteristics. STDP modulates synapse weight based on the activities of the so-called pre- and postsynaptic neurons [11]. The spikes from both preneuron and postneuron arrive at the synapse occasionally in the opposite direction [7]. In STDP, the change of the synaptic weight is the function of relative neuron spike timing Δt ($\Delta t = t_{pre} - t_{post}$), where t_{pre} is the time when the presynaptic neuron spike arrives and t_{post} is the time when the postsynaptic neuron spike arrives [4]. In a typical STDP behavior, if postsynaptic neuron spike arrives after presynaptic neuron spike ($\Delta t < 0$), the synaptic weight increases. If postsynaptic neuron spike arrives before presynaptic neuron spike ($\Delta t > 0$), the synaptic weight decreases. In electronic synapse based on memristor, voltage spikes or pulses are applied on the memristor through the two electrodes, which modulates the conductance of the memristor, and the change of conductance is related to the relative timing of voltage spikes or pulses. Memristors can realize STDP function which is similar with that of biological synaptic systems, which is shown in **Figure 2** [4].
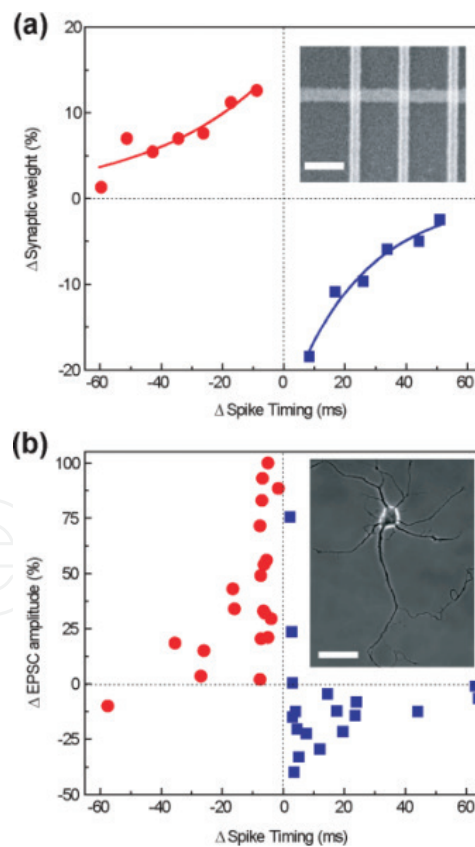

Figure 2. (a) The relationship between change of the memristor synaptic weight and the relative timing Δt of the neuron spikes. The synaptic change was normalized to the maximum synaptic weight. Inset (a): SEM image of the crossbar structure of memristors. (b) The relationship between the change in excitatory postsynaptic current (EPSC) of rat hippocampal neurons after repetitive correlated spiking (60 pulses at 1 Hz) and relative spike timing. The figure was reconstructed with permission from Ref. [8, 12]. Inset (b) is the phase contrast image of a hippocampal neuron, which was adapted with permission from Ref. [4, 13, 26].

STDP have been intensively investigated in the different memristors with different materials. The memristors are usually composed of two electrodes and memristive materials sandwiched between two electrodes. Metals such as Au, Pt, Ag, Cu, conductive nitrides such as TiN, and conductive oxides such as ITO are usually used as the materials of electrodes. The memristive materials can be grouped into binary oxides, ternary and more complex oxides, polymer, and other kind of materials.

The STDP of binary memristive materials such as TiO_x [6], WO_x [3], Al_2O_3/TiO_2 [14], CeO_x [15], TaO_x/Ta_2O_5 [16], and HfO_2 [17, 18] have been investigated very intensively; Seo et al. tested the STDP function of the memristor based on TiO_x, and they demonstrated the potential of such memristor as electronic synapses in neuromorphic network. The results are shown in **Figure 3**. Matveyev et al. demonstrated the STDP functionality of HfO_2-based memristor with the structure of $TiN/HfO_2/Pt$ [17]. The function relationship between the relative change of the conductance ΔG and the spikes' delay time Δt was obtained from the 4-nm-thick HfO_2 40×40 nm^2 device, which is shown in **Figure 4**. Tan et al. conducted investigation on the memristor with the structure of $Pt/WO_3/Pt$. The STDP behavior was demonstrated in such WO_3-based memristor, which is illustrated in **Figure 5(b)** [3]. Wang et al. carried out investigation on memristor device of $Pt/HfO_x/ZnO_x/TiN$. The STDP characteristics of the memristors were measured with voltage pulses with the amplitude of the $V^-/V^+ = -1.0$ V/1.0 V. Those voltage pulses were applied on the top electrode and bottom electrode as presynaptic and postsynaptic spikes. The relationship between the relative change of the synaptic weight and relative spike timing is illustrated in **Figure 6(b)**, which is basically consistent with the STDP behavior of biological synapse.

Memristors based on ternary and more complex oxides such as $BiFeO_3$ [19], InGaZnO [20], and so on, were also investigated.

Wang et al. reported that STDP was observed in the memristors based on amorphous InGaZnO. As shown in **Figure 7(c, d)**, a pair of voltage spikes with amplitude of $V^+/V^- = 5$
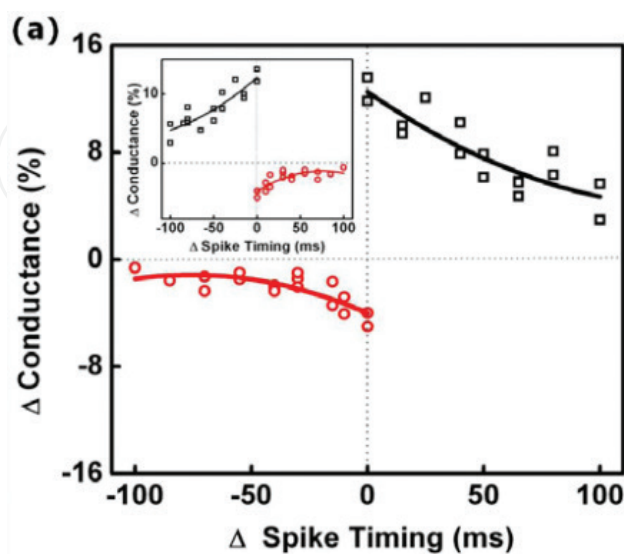

Figure 3. STDP synaptic characteristic of the memristor. Inset shows the anti-STDP synaptic characteristic of the memristor [6].
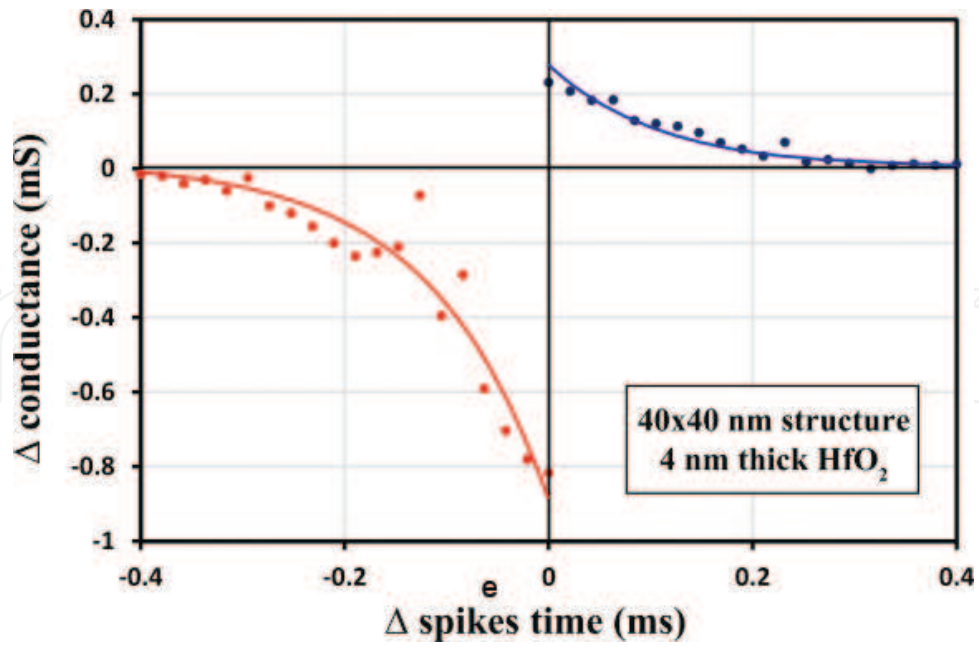
Figure 4. Asymmetric STDP characteristic emulated in crossbar 4-nm-thick, 40×40 nm^2 HfO$_2$-based memristors [17].
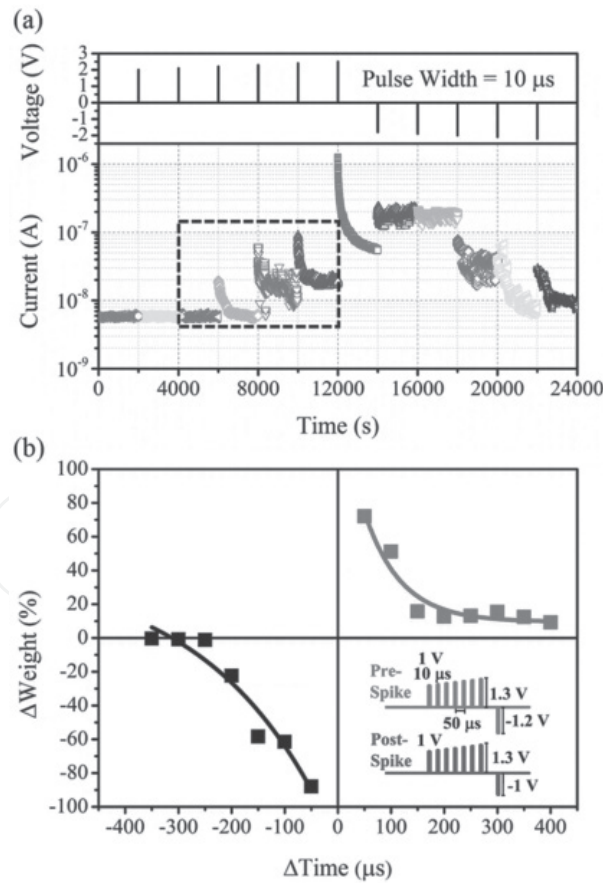

Figure 5. Experimental results of the STDP characteristic of Pt/WO$_3$/Pt memristor. (a) Current decay after the application of a sequence of positive and negative pulses was measured with reading voltage with the amplitude of 0.05 V. The transition from volatile to nonvolatile is indicated in the dotted square. (b) The relationship between the change of the synaptic weight and the relative timing of the prespike and postspike. Inset (b): waveform of prespike and postspike [3].
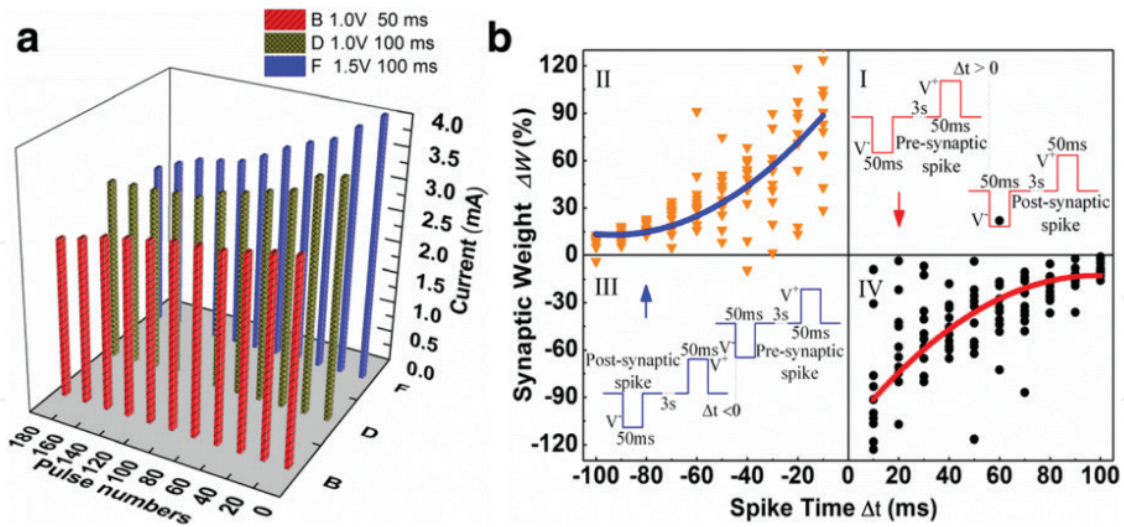
Figure 6. Nonlinear transmission characteristics and STDP of the memristor device. (a) Response of a memristor to different pulses; (b) emulation of STDP characteristics of memristor with the structure of Pt/HfO$_x$/ZnO$_x$/TiN—the relationship between the relative change of the memristor synaptic weight (ΔW) and the relative spike timing (Δt). And the solid line is the exponential fitting curve to the experimental data. The insets (b): schematics of various spikes.
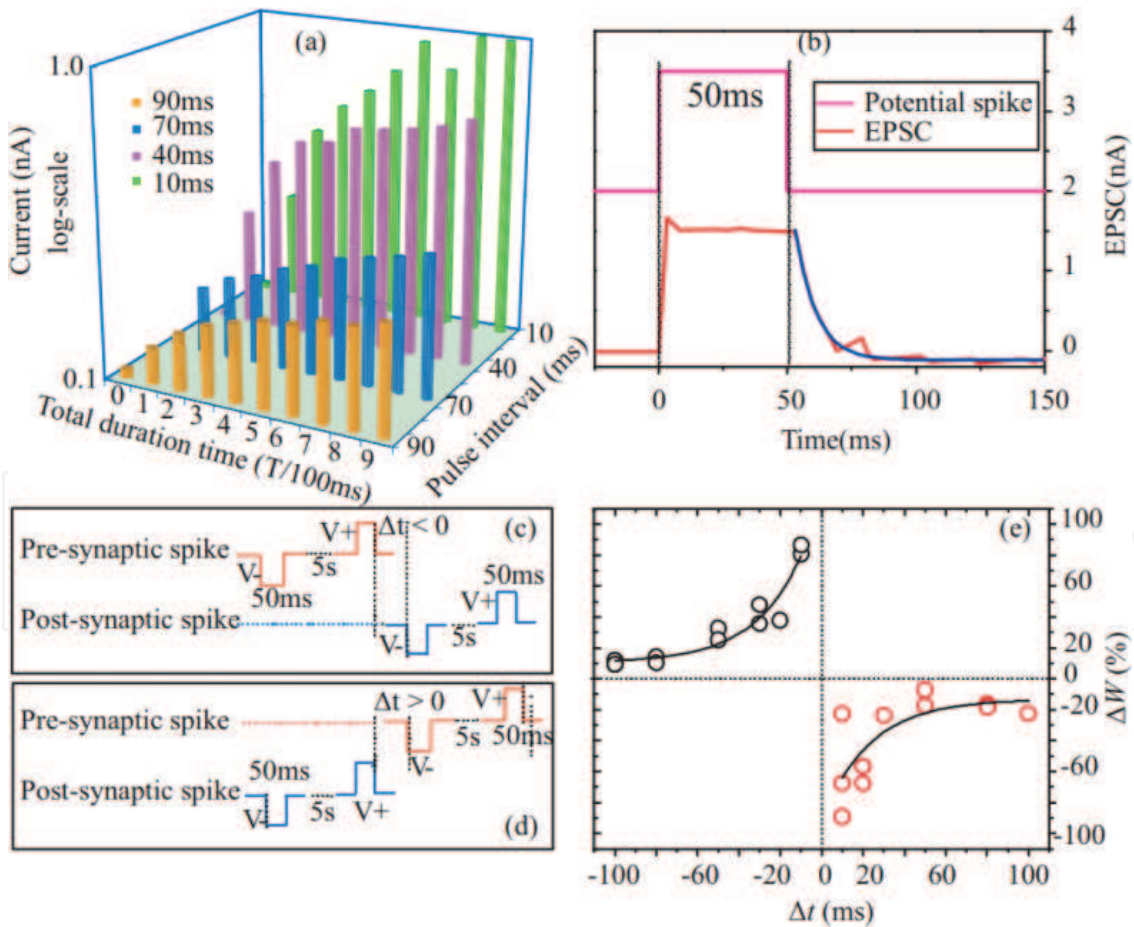

Figure 7. Demonstration of STDP characteristics of memristor. (a) The variation of the current with the interval of voltage pulses. (b) The formation and decay of spike-induced EPSC. (c and d) The preneuron spike and postneuron spike applied on the memristor for STDP. (e) The relationship between the relative change of the memristor synaptic weight (ΔW) and the relative spike timing (Δt). The exponential fitting results for the experimental data are illustrated by the solid lines in the graph.

V/−5 V was applied on the two terminals of the memristors with relative timing Δt to test the STDP characteristics. As shown in **Figure 7(e)**, the ΔW changed with Δt, which is a typical STDP characteristic of biological synapses.

The STDP behavior was also observed in polymer such as poly(3,4-ethylenedioxythiophene): poly(styrenesulfonate) (PEDOT:PSS) [21], EV(ClO$_4$)$_2$/BTPA-F [22], and so on. Li et al. imitated the STDP of Ag/PEDOT:PSS/Ta structure [23]. A pair of temporally correlated voltage pulses with amplitudes V$^+$/V$^-$ = 2 V/−2 V was used as presynaptic spikes and postsynaptic spikes, which was applied to the memristors, respectively. The change of the synaptic weights related to the precise timing between pre- and postsynaptic spikes is shown in **Figure 8(c)**.

In addition, the investigations on the STDP of the memristors based on other kind of materials such as Si/Ag mixture [4], polycrystal CH$_3$NH$_3$PbI$_3$ [24], have also been conducted.

Some factors in the STDP measurements can change some characteristics of the STDP, for example, the waveform of voltage spikes used to imitate the presynaptic neuron spike and postsynaptic neuron spike influences the STDP behavior significantly. It has been reported that the STDP function can be strongly influenced by the shape of the input voltage spikes [25]. The shape of voltage spike generated from presynaptic neuron is the same with that generated from postsynaptic neuron. Zamarreño-Ramos et al. investigated the influence of the shape of the voltage spikes (spk(t)) on STDP learning function ξ (ΔT). The results are shown in **Figure 9**. The results reveals that the voltage spikes with a narrow short positive pulse of large amplitude and a longer relaxing slowly decreasing negative tail are needed in order to obtain the STDP function similar with the behavior of the biological synapses [25].
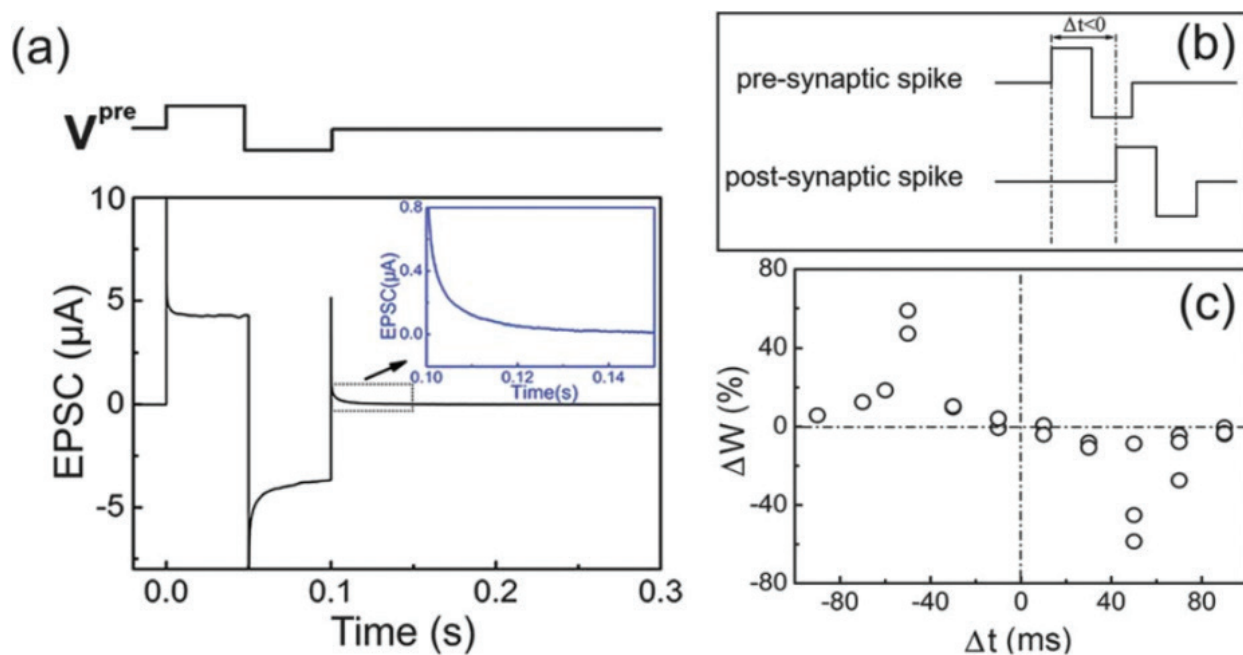

Figure 8. Simulation of STDP. (a) EPSC. The preneuron spike was V$^+$/V$^-$ = 2 V/−2 V. The current value gradually decayed back to zero within 50 ms after the spike. A pair of temporally correlated pulses with amplitudes V$^+$/V$^-$ = 2 V/−2 V was applied to the TE and BE as preneuron spikes and postneuron spikes, respectively. (b) Δt is the interval between the beginning of the preneuron spikes and the beginning of the postneuron spikes. (c) STDP characteristics. The relationship between the change of synaptic weight and Δt defined in (b).
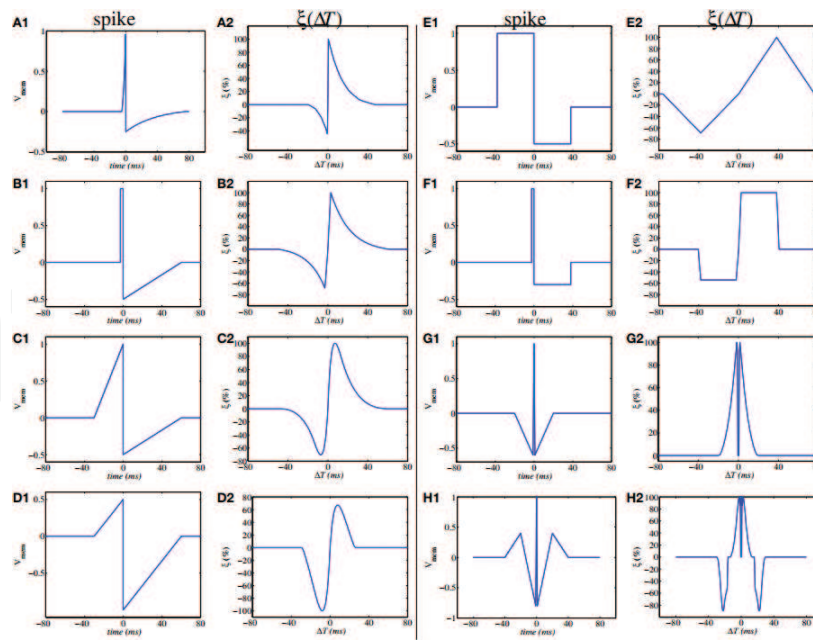
Figure 9. Illustration of influence of shape of waveform of the voltage spikes on the STDP learning function $\xi(\Delta T)$. X1 is spike waveform applied on the memristor, and X2 is resulting STDP learning function, where X goes from A to H [25].

Cederström et al. investigated the role of device hysteresis characteristic of the memristors played in the operation of its STDP function. Hysteresis characteristics of memristors based on $BiFeO_3$, Ag/Si, TiO_2, and chalcogenide (PCM) were compared. STDP characteristics were simulated with different models of different memristors, and the results are shown in **Figure 10**. The influence of switching characteristics on the operating region used for STDP was discussed. A smooth switching characteristics leads to a much wider operation region, and a steep switching characteristics leads to a much narrower operation region [26].

Du et al. reported that the learning time constant can be adjusted through changing the duration of the voltage spikes. The scheme of the voltage spikes is shown in **Figure 11**, and pulse width (t_p) is one of the parameters of the voltage spikes. The range of the delay time Δt where the normalized current is larger than 50% is called learning window. As shown in **Figure 12**, learning window decreases from 25 ms to 125 µs with the decrease of pulse width (t_p) from 10 ms to 50 µs. In addition, energy consumption of the memristors was also discussed in this work, the authors showed that energy consumption of the Au/BFO/Pt/Ti memristor is 4.7 pJ. A method to reduce the energy consumption was proposed and tested, and the results indicate by decreasing the pulse width (t_p) energy consumption can be reduced to 4.5 pJ.

Xiao et al. reported the STDP characteristics of the memristor with the structure of Au/polycrystal $CH_3NH_3PbI_3$/ITO/PEDOT:PSS. Different waveforms were used as presynaptic neuron voltage spike and postsynaptic neuron voltage spike, which are shown in **Figure 13(b–e)**. Four different kinds of STDP characteristics, including asymmetric Hebbian rule, asymmetric anti-Hebbian rule, symmetric Hebbian rule, and symmetric anti-Hebbian rule, were obtained corresponding to four different waveforms applied to the memristor as shown in **Figure 13(f–i)**. And the four kinds of STDP behaviors were fit by different equations [24].
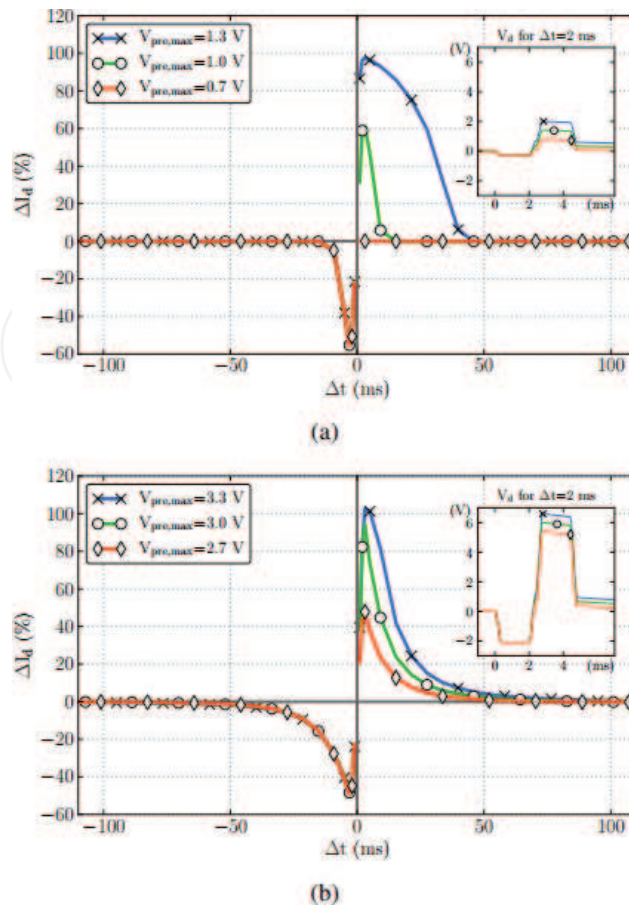
Figure 10. STDP simulations by the implementation of SPICE models, and for each Δt, a sequence of 60 pulses has been used to change the conductance. The waveforms used were adapted (a) for the TiO_2 device model and (b) for our BFO device model [26].
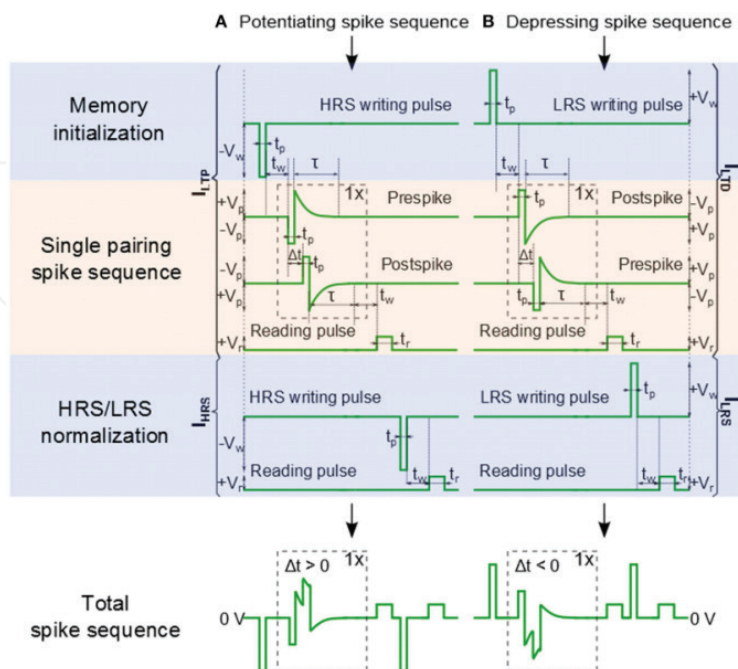

Figure 11. Schematic of the waveforms for memristor initialization, single pairing STDP, and memory consolidation. (A) A pre-post spike order is used for long-term potentiation (LTP). (B) A post-pre spike order is used for long-term depression (LTD) [19].
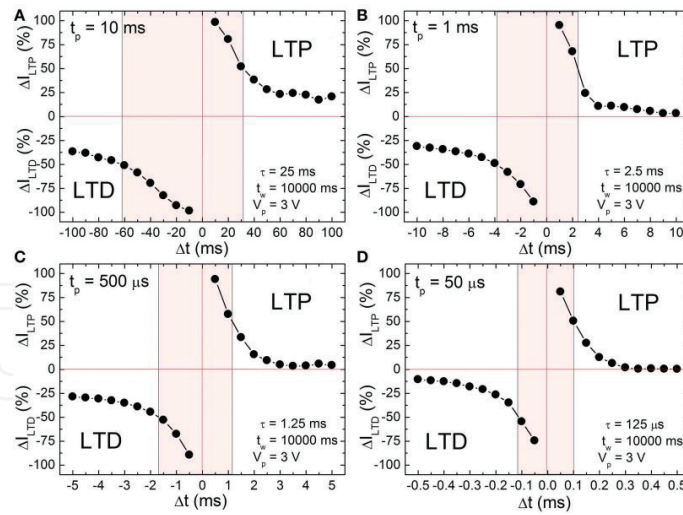
Figure 12. STDP characteristics of a BFO-based memristor with single pairing pulse width (A) t_p = 10 ms, (B) t_p = 1 ms, (C) t_p = 500 μs, and (D) t_p = 50 μs, measurement waiting time t_w = 10,000 ms, pulse amplitude V_p = 3.0 V, reading pulse amplitude V_r = +2.0 V, and reading pulse width t_r = 100 ms. The memristor was preset in HRS and LRS with a writing pulse amplitude of V_w = −8.0 V and V_w = +8.0 V, respectively [19].
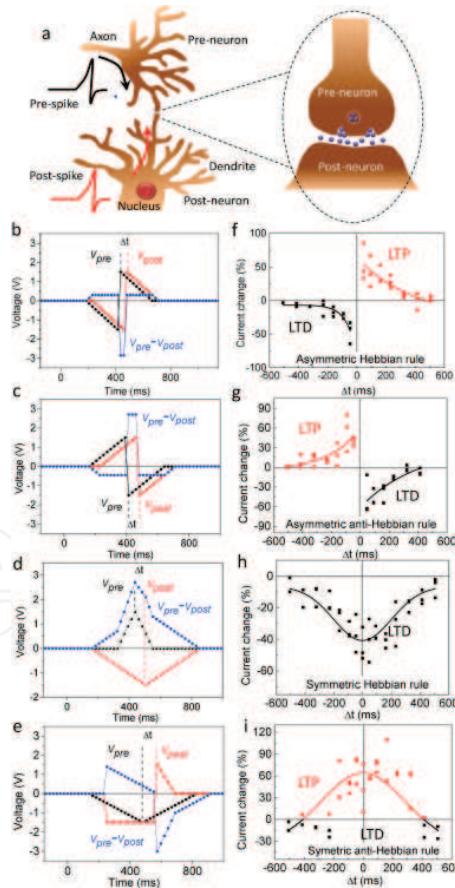

Figure 13. STDP characteristics of memristor: (a) schematics of a biological synapse. The voltage spikes for (b) asymmetric Hebbian rule, (c) asymmetric anti-Hebbian rule, (d) symmetric Hebbian rule, and (e) symmetric anti-Hebbian rule. (f-i) The current change with the applying of corresponding voltage spikes. The conductance of the synaptic device was read with a reading pulse amplitude of −0.75V before and after the applying of the voltage spikes with the interval of 3 s [24].

$$\Delta W = A \exp(-\tfrac{\Delta}{\tau}) + W_0 \tag{2}$$

$$\Delta W = A \exp(-\tfrac{\Delta t^2}{2\tau^2}) + W_0 \tag{3}$$

Prezioso et al. investigated the STDP characteristics of the memristor with the structure of Pt/Al$_2$O$_3$/TiO$_{2-x}$/Ti/Pt. Three pairs of preneuron spike and postneuron spike with different waveforms, which are shown in **Figure 14(a–c)**, were applied on the memristor. Three different STDP behaviors were observed, which are illustrated in **Figure 14(g–i)**. The results demonstrated the dependence of STDP window on the waveform of preneuron spike and postneuron spike. The investigation regarding the influence of the initial conductance (G_0) on the STDP behavior was also conducted. In this set of tests, the waveform shown in **Figure 14(a)** was used. The STDP functions for different initial conductance G_0 = 25, 50, 75, and 100 µS were measured and compared. The results shown in **Figure 15** indicate the influence of the switching dynamics' saturation of the memristors on the STDP property. All the memristors have their own dynamic range of the conductance. When G_0 is close to its maximum value, the increase of the conductance is very low. And when G_0 is close to its minimum value, the decrease of the conductance is very low [14].
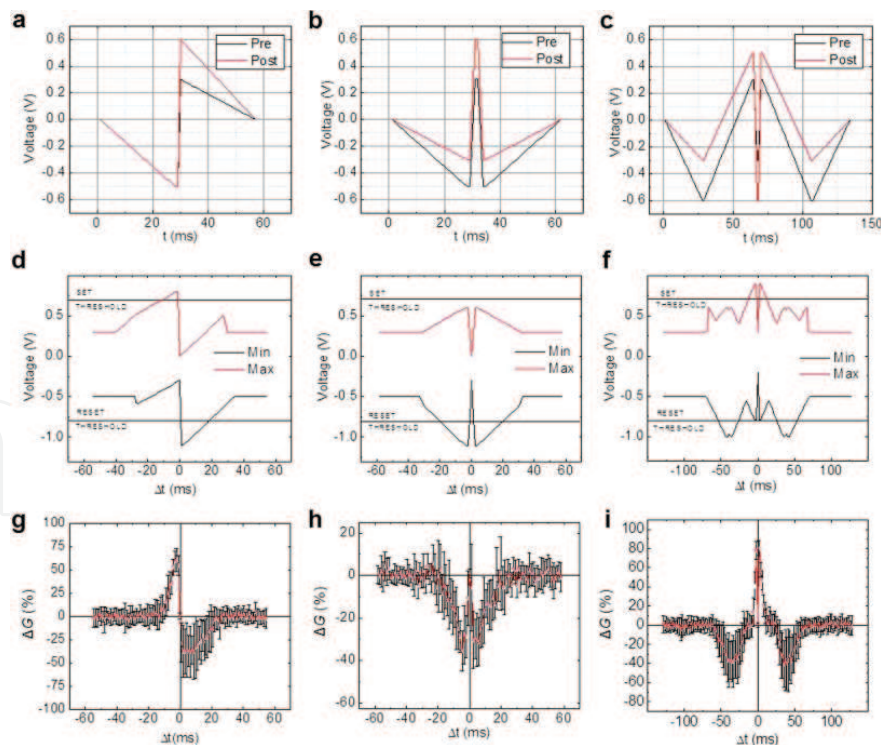

Figure 14. Experimental results for STDP characteristics. (a–c) The shapes of presynaptic and postsynaptic voltage pulses, marked by black lines and red lines, respectively (d–f) The time maxima and minima of the net voltage applied to the memristor, as functions of the time interval Δt between the pre- and postsynaptic pulses. (g–i) STDP characteristic of the memristors: the relationship between the changes of memristor's conductance and Δt. The initial memristor conductance G_0 was always set to about 33 µS in all the experiments mentioned above [14].
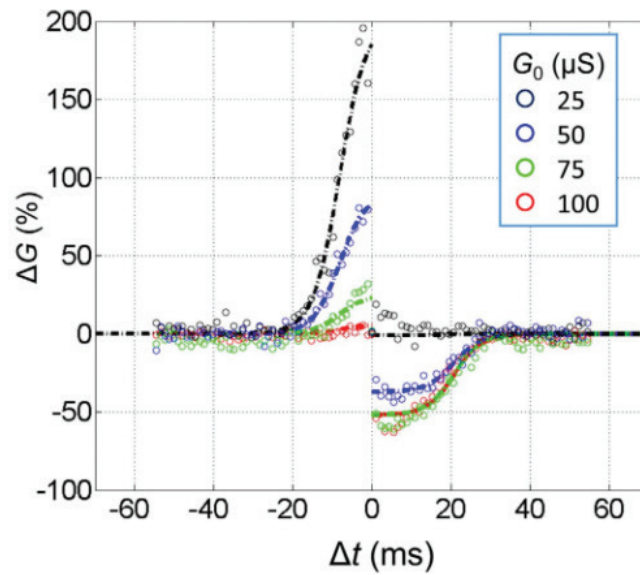
Figure 15. The experimentally measured STDP window function with several initial values G_0 = 25, 50, 75, and 100 μs together with the results of its fitting with equations (dash-dot lines) [14].

3. Conclusions

In summary, the STDP characteristics have been observed in different memristors based on different kinds of materials, which make memristors become promising in the bio-inspired neuromorphic application. Great efforts have also been made in the investigation on the influence factors of the STDP characteristics such as device hysteresis characteristic and the waveform of the voltage pulses applied to the memristor as preneuron voltage spike and postneuron voltage spike. Different kinds of waveform were used, and different kinds of STDP characteristics were observed.

Acknowledgements

Author details

Yao Shuai*, Xinqiang Pan and Xiangyu Sun

*Address all correspondence to: yshuai@uestc.edu.cn

State Key Laboratory of Electronic Thin Films and Integrated Devices, University of Electronic Science and Technology of China, Chengdu, China

References

[1] Gibney E. Artificial intelligence. What Google's winning Go algorithm will do next. Nature. 2016;**531**:284-285

[2] Snider GS. Spike-timing-dependent learning in memristive nanodevices. IEEE, New York, NY 10017 USA In: 2008 IEEE International Symposium on Nanoscale Architectures. Anaheim, CA. 2008. pp. 85-92

[3] Tan ZH, Yang R, Terabe K, Yin XB, Zhang XD, Guo X. Synaptic metaplasticity realized in oxide memristive devices. Advanced Materials. 2016;**28**:377-384

[4] Jo SH, Chang T, Ebong I, Bhadviya BB, Mazumder P, Lu W. Nanoscale memristor device as synapse in neuromorphic systems. Nano Letters. 2010;**10**:1297-1301

[5] Chua LO. Memristor—the missing circuit element. IEEE Transactions on Circuit Theory. 1971;**18**:507-519

[6] Seo K, Kim I, Jung S, Jo M, Park S, Park J, et al. Analog memory and spike-timing-dependent plasticity characteristics of a nanoscale titanium oxide bilayer resistive switching device. Nanotechnology. 2011;**22**:254023

[7] Yu SM, Wu Y, Jeyasingh R, Kuzum DG, Wong HSP. An electronic synapse device based on metal oxide resistive switching memory for neuromorphic computation. IEEE Transactions on Electron Devices. 2011;**58**:2729-2737

[8] Jang JW, Park S, Jeong YH, Hwang H. ReRAM-based synaptic device for neuromorphic computing. IEEE, New York, NY 10017 USA. In: 2014 IEEE International Symposium on Circuits and Systems (ISCAS). Melbourne, Australia. 2014. pp. 1054-1057

[9] Hu SG, Liu Y, Liu Z, Chen TP, Wang JJ, Yu Q, et al. Associative memory realized by a reconfigurable memristive Hopfield neural network. Nature Communications. 2015;**6**:7522

[10] Prezioso M, Merrikh-Bayat F, Hoskins BD, Adam GC, Likharev KK, Strukov DB. Training and operation of an integrated neuromorphic network based on metal-oxide memristors. Nature. 2015;**521**:61-64

[11] Mostafa H, Khiat A, Serb A, Mayr CG, Indiveri G, Prodromakis T. Implementation of a spike-based perceptron learning rule using TiO_{2-x} memristors. Frontiers in Neuroscience. 2015;**9**:357

[12] Bi GQ, Poo MM. Synaptic modifications in cultured hippocampal neurons: Dependence on spike timing, synaptic strength, and postsynaptic cell type. Journal of Neuroscience. 1998;**18**:10464-10472

[13] Kaech S, Banker G. Culturing hippocampal neurons. Nature Protocols. 2006;**1**:2406-2415

[14] Prezioso M, Merrikh Bayat F, Hoskins B, Likharev K, Strukov D. Self-adaptive spike-time-dependent plasticity of metal-oxide memristors. Scientific Reports. 2016;**6**:21331

[15] Hsieh C-C, Roy A, Chang Y-F, Shahrjerdi D, Banerjee SK. A sub-1-volt analog metal oxide memristive-based synaptic device with large conductance change for energy-efficient spike-based computing systems. Applied Physics Letters. 2016;**109**:223501

[16] Kim S, Choi S, Lu W. Comprehensive physical model of dynamic resistive switching in an oxide memristor. ACS Nano. 2014;**8**:2369-2376

[17] Matveyev Y, Kirtaev R, Fetisova A, Zakharchenko S, Negrov D, Zenkevich A. Crossbar nanoscale HfO_2-based electronic synapses. Nanoscale Research Letters. 2016;**11**:147

[18] Covi E, Brivio S, Serb A, Prodromakis T, Fanciulli M, Spiga S. HfO_2-based memristors for neuromorphic applications. IEEE, New York, NY 10017 USA; In: IEEE International Symposium on Circuits and Systems. Montreal, Canada. 2016. pp. 393-396

[19] Du N, Kiani M, Mayr CG, You T, Burger D, Skorupa I, et al. Single pairing spike-timing dependent plasticity in $BiFeO_3$ memristors with a time window of 25 ms to 125 μs. Frontiers in Neuroscience. 2015;**9**:227

[20] Wang ZQ, Xu HY, Li XH, Yu H, Liu YC, Zhu XJ. Synaptic learning and memory functions achieved using oxygen ion migration/diffusion in an amorphous InGaZnO memristor. Advanced Functional Materials. 2012;**22**:2759-2765

[21] Chen Y, Liu G, Wang C, Zhang WB, Li RW, Wang LX. Polymer memristor for information storage and neuromorphic applications. Materials Horizons. 2014;**1**:489-506

[22] Liu G, Wang C, Zhang W, Pan L, Zhang C, Yang X, et al. Organic biomimicking memristor for information storage and processing applications. Advanced Electronic Materials. 2016;**2**:1500298

[23] Li S, Zeng F, Chen C, Liu H, Tang G, Gao S, et al. Synaptic plasticity and learning behaviours mimicked through Ag interface movement in an Ag/conducting polymer/Ta memristive system. Journal of Materials Chemistry C. 2013;**1**:5292

[24] Xiao Z, Huang J. Energy-efficient hybrid perovskite memristors and synaptic devices. Advanced Electronic Materials. 2016;**2**:1600100

[25] Zamarreno-Ramos C, Camunas-Mesa LA, Perez-Carrasco JA, Masquelier T, Serrano-Gotarredona T, Linares-Barranco B. On spike-timing-dependent-plasticity, memristive devices, and building a self-learning visual cortex. Frontiers in Neuroscience. 2011;**5**:26

[26] Cederstrom L, Starket P, Mayr C, Shuai Y, Schmidt H, Schuffny R. A model based comparison of $BiFeO_3$ device applicability in neuromorphic hardware. IEEE, New York, NY 10017 USA; In: 2013 IEEE International Symposium on Circuits and Systems (ISCAS). Beijing, China. 2013. pp. 2323-2326